Energy Fuels 2010, 24, 5273–5280 · DOI:10.1021/ef100679e
Published on Web 08/11/2010

energy&fuels
article

Isothermal versus Non-isothermal Adsorption−Desorption Cycling of Triamine-Grafted Pore-Expanded MCM-41 Mesoporous Silica for CO_2 Capture from Flue Gas

Youssef Belmabkhout and Abdelhamid Sayari*

Department of Chemistry, University of Ottawa, Ottawa, Ontario K1N 6N5, Canada

Received June 2, 2010. Revised Manuscript Received August 2, 2010

CO_2 adsorption−desorption isotherms for triamine-grafted pore-expanded mesoporous silica (TRI-PE-MCM-41) were measured up to 25 bar using the same adsorption and pretreatment temperatures at 298, 323, and 343 K and compared to CO_2 adsorption data for 13X zeolite, aminated metal organic framework (Zn-Atz MOF), and Darco activated carbon (Darco-AC). Cyclic isothermal adsorption−desorption measurements of pure CO_2 and a 10:90 CO_2/N_2 mixture were carried out using vacuum swing (VS) and concentration swing (CS) regeneration modes at 298 and 343 K, in dry and humid conditions, and compared to cyclic non-isothermal desorption measurements, i.e., temperature swing (TS) and temperature-vacuum swing (TVS) regeneration operations. In addition to high CO_2 selectivity, it was found that, in comparison to the three other adsorbents, TRI-PE-MCM-41 exhibited higher CO_2 uptake in the presence of a 10:90 CO_2/N_2 mixture in both dry and humid conditions. Cyclic experiments using VS regeneration mode at 343 K gave a similar CO_2 uptake as the TS regeneration mode. Similar to liquid-phase CO_2 absorption, SO_2 had a deleterious effect on CO_2 adsorption.

Downloaded via CASE WESTERN RESERVE UNIV on July 1, 2021 at 20:42:34 (UTC).
See https://pubs.acs.org/sharingguidelines for options on how to legitimately share published articles.

1. Introduction

Fossil fuel power plants represent a major contributor to anthropogenic CO_2 emissions. Because of their adverse effect on global climate change, reducing such emissions has become a major challenge facing modern society.[1,2] Carbon capture and sequestration (CCS) is one of the key options for achieving this goal.[3,4] The capture (separation) step is estimated to represent 75% of the overall CCS cost.[5] Among the possible technologies for CO_2 removal, adsorption is recognized to be an energy-efficient, cost-effective method.[6,7] The CO_2 selectivity is one of the key parameters affecting the performance of the process and, thus, the cost of separation. As far as CO_2 removal from flue gas is concerned, in addition to high selectivity, the adsorbent should possess other attributes, such as (i) high adsorption capacity in the 298−343 K temperature range at atmospheric pressure, as well as high adsorption rate, (ii) ease of regeneration under mild conditions, (iii) high stability, and (iv) tolerance to moisture and other impurities in the feed.

A large number of adsorbents were investigated for CO_2 removal, including 13X zeolite,[8,9] activated carbons,[10,11] periodic mesoporous silicas,[12] as well as metal organic frameworks (MOFs).[13−16] In recent years, amine-modified solid

*To whom correspondence should be addressed. E-mail: abdel.sayari@uottawa.ca.

(1) Ko, D.; Siriwardane, R.; Biegler, L. T. Optimization of pressure swing adsorption and fractionated vacuum pressure swing adsorption processes for CO_2 capture. *Ind. Eng. Chem. Res.* **2005**, *44*, 8084–8094.
(2) Yang, W. C.; Hoffman, J. Exploratory design on reactor configuration for carbon dioxide capture form conventional power plants employing regenerable solid adsorbents. *Ind. Eng. Chem. Res.* **2009**, *48*, 341–351.
(3) Audus, H. Greenehouse gas mitigation technology: An overview of the CO_2 capture and sequestration studies and further activities of the IEA greenhouse gas R&D programme. *Energy* **1997**, *22*, 217–221.
(4) Meisen, A.; Shuai, X. Research and development issues in CO_2 capture. *Energy Convers. Manage.* **1997**, *38*, S37–S42.
(5) Zhang, J.; Webley, P. A.; Xiao, P. Effect of process paramaters on power requirements of vacuum swing adsorption technology for CO_2 capture from flue gas. *Energy Convers. Manage.* **2008**, *49*, 346–356.
(6) Aaron, D.; Tsouris, C. Separation of CO_2 from flue gas: A review. *Sep. Sci. Technol.* **2005**, *40*, 321–348.
(7) Sjostrom, A.; Krutka, H. Evaluation of solid sorbents as a retrofit technology for CO_2 capture. *Fuel* **2010**, *89*, 1298–1306.
(8) Xiao, P.; Zhang, J.; Webley, P. A.; Li, G.; Singh, R.; Todd, R. Capture of CO_2 form flue gas streams with zeolite 13X by vacuum-pressure swing adsorption. *Adsorption* **2008**, *14*, 575–582.
(9) Ho, M. T.; Allinson, G. W.; Wiley, D. E. Reducing the cost of CO_2 capture from flue gases using pressure swing adsorption. *Ind. Eng. Chem. Res.* **2008**, *47*, 4883–4890.
(10) Himeno, S.; Komatsu, T.; Fujita, S. Development of a new effective biogas adsorption storage technology. *Adsorption* **2005**, *11*, 899–904.
(11) Zhou, L.; Wu, J.; Li, M.; Wu, Q.; Zhou, Y. Prediction of multicomponent adsorption equilibrium of gas mixtures including supercritical components. *Chem. Eng. Sci.* **2005**, *60*, 2833–2844.
(12) Belmabkhout, Y.; Serna-Guerrero, R.; Sayari, A. Adsorption of CO_2 from dry gases on MCM-41 silica at ambient temperature and high pressure 1: Pure CO_2 adsorption. *Chem. Eng. Sci.* **2009**, *64*, 3721–3728.
(13) Babarao, R.; Jiang, J.; Sandler, S. I. Molecular simulation for adsorptive separation of CO_2/CH_4 mixture in metal-exposed, catenated, and charged metal organic frameworks. *Langmuir* **2009**, *25*, 5239–5247.
(14) Cheng, Y.; Kondo, A.; Noguchi, H.; Kajiro, H.; Urita, K.; Ohba, T.; Kaneko, K.; Kanoh, H. Reversible structural change of Cu-MOF on exposure to water and its CO_2 adsorptivity. *Langmuir* **2009**, *25*, 4510–4513.
(15) Bae, Y. S.; Mulfort, K. L.; Frost, H.; Ryan, P.; Punatahnam, S.; Braodbelt, L. J.; Hupp, J. T.; Snurr, Q. R. Separation of CO_2 and CH_4 using mixed-ligand metal−organic frameworks. *Langmuir* **2008**, *24*, 8592–8598.
(16) Caskey, S. R.; Wong-Foy, A. G.; Matzger, A. J. Dramatic tuning of carbon dioxide uptake via metal substitution in a coordination polymer with cylindrical pores. *J. Am. Chem. Soc.* **2008**, *130*, 10870–10871.
(17) Harlick, P. J. E.; Sayari, A. Application of pore-expanded mesorporous silica 5. Triamine grafted material with exceptional CO_2 dynamic and equilibrium adsorption performance. *Ind. Eng. Chem. Res.* **2007**, *46*, 446–458.
(18) Belmabkhout, Y.; Sayari, A. Effect of pore expansion and amine functionalization of mesoporous silica on CO_2 adsorption over a wide range of pressure and temperature. *Adsorption* **2009**, *15*, 318–328.
(19) Hicks, J. C.; Drese, J. D.; Fauth, D. J.; Gray, M. L.; Qi, G.; Jones, C. W. Designing adsorbents for CO_2 capture from flue gas—Hyperbranched aminosilicas capable of capturing CO_2 reversibly. *J. Am. Chem. Soc.* **2008**, *130*, 2902–2903.

sorbents have also attracted increasing attention.[17−31] Dependent upon the adsorbent properties, solid−gas adsorption operations may be carried out using (i) isothermal regeneration modes, such as pressure swing adsorption (PSA), including vacuum (VSA) or concentration swing adsorption (CSA), or (ii) non-isothermal regeneration modes, such as temperature swing adsorption (TSA) or a combination of temperature and pressure gradients, i.e., PTSA or VTSA. The nature of the adsorbate−adsorbent interactions plays a major role in establishing the appropriate driving force required for regeneration. In TSA, the gases adsorbed are desorbed by increasing the temperature, whereas in PSA, desorption takes place via depressurization, and in TPSA, desorption is induced by a combination of high temperature and low pressure. Because for amine-containing adsorbents, the CO_2−adsorbent interactions are chemical in nature, heat-driven regeneration modes (TS and TVS) are likely to be the most appropriate. In an earlier report,[29] we showed that TRI-PE-MCM-41 exhibits interesting properties in terms of CO_2 selectivity over N_2, O_2, CH_4, and H_2. Moreover, as shown in Figure S1 in the Supporting Information, TRI-PE-MCM-41 is a highly stable material when TS or TVS regeneration mode is used.[32] In addition, measurements of cyclic adsorption capacity using TVS and TS regeneration modes with adsorption at 323 K and desorption at 363 K showed that, in the presence of pure CO_2 as well as a 10:90 CO_2/N_2 mixture, in both dry and humid conditions, TRI-PE-MCM-41 outperformed 13X zeolite and metal organic framework (Zn-Atz MOF) in terms of overall adsorption capacity (Figures S2−S5 in the Supporting Information). Although high CO_2 uptake of ca. 6 and 7 wt % was obtained using TS and TVS cycling for a 10:90 CO_2/N_2 mixture, these procedures may not be suitable for rapid cycling because of the lengthy heating and cooling operations. An exhaustive literature study showed that only the amine-impregnated class of materials was investigated using heat-free regeneration modes.[33−35] Despite the large number of contributions devoted to CO_2 adsorption over amine-containing materials,[36] and despite the utmost importance of fast cycling for CO_2 capture and removal, to the best of our knowledge, no studies showed the feasibility of using heat-free regeneration modes, i.e., pressure (vacuum) swing or concentration swing, for amine-grafted materials.

As a part of our effort to optimize the performance of TRI-PE-MCM-41 for CO_2 removal from various gas streams, this study provides new insight into the suitability of amine-bearing adsorbent of CO_2 removal from flue gas using PSA (VSA). The CO_2 adsorption capability of TRI-PE-MCM-41 in comparison to 13X, Zn-Atz MOF, and Darco activated carbon (Darco-AC) was investigated using concentration and pressure gradients for regeneration, with adsorption, desorption, and pretreatment taking place at the same temperature. Isothermal cycling will be denoted VS(T) or CS(T), where T indicates the adsorption and desorption temperature in Kelvin, whereas the desorption pressure is 0.1 and 1 bar for VS and CS operations, respectively. As for non-isothermal cycling operations, they will be designated, for example, as TS ($T_a-P_d-T_d$), where T_a and T_d indicate the adsorption and desorption temperatures in Kelvin and P_d is the desorption pressure in bar.

2. Experimental Section

2.1. Materials. The detailed preparation procedure and structural characteristics of TRI-PE-MCM-41 may be found elsewhere.[17,18] The Brunauer−Emmett−Teller (BET) surface area, pore size, and pore volume of TRI-PE-MCM-41 were 367 m^2/g, 9.4 nm, and 0.87 cm^3/g. The nitrogen content as determined by elemental analysis was ca. 7 mmol/g. 13X zeolite (658 m^2/g; 0.31 cm^3/g) and Darco-AC (1657 m^2/g; 0.13 nm; 1.5 cm^3/g) were supplied by Sigma-Aldrich.

Zn-Atz MOF was prepared following the procedure of Vaidhyanathan et al.[31] and did not exhibit any porosity. Briefly, 1.25 g of H_2O and 7.5 mL of methanol were mixed with 0.25 g of zinc carbonate, 1 g of 3-amino-1,2,4-triazole, and 0.25 g of oxalic acid. The mixture was heated in an autoclave at 453 K for 2 days. The material was cooled, filtered, washed twice with water, and dried in air. All reagents were supplied by Aldrich and used as received. Carbon dioxide (99.99%), nitrogen (99.999%), helium (99.999%), and carbon dioxide (10%) in nitrogen were supplied by BOC Canada.

2.2. CO_2 Adsorption Equilibria and Cyclic Adsorption. Pure CO_2 equilibrium adsorption measurements as well as non-equilibrium cyclic measurements were performed using a Rubotherm gravimetric−densimetric apparatus (Bochum, Germany). The equilibrium adsorption−desorption measurements were carried out using samples pretreated under vacuum

(20) Chaffee, A. L.; Knowles, G. P.; Liang, Z.; Zhang, J.; Xiao, P.; Webley, P. A. CO_2 capture by adsorption: Materials and process development. *Int. J. Greenhouse Gas Control* **2007**, *1*, 11.
(21) Yue, M. B.; Sun, L. B.; Cao, Y.; Wang, Y.; Wang, Z. J; Zhu, J. H. Efficient CO_2 capturer derived from as-synthetized MCM-41 modified with amine. *Chem.—Eur. J.* **2008**, *14*, 3442–3451.
(22) Lu, C.; Bai, H.; Wu, B.; Su, F.; Hwang, J. F. Comparative study of CO_2 capture by carbon nanotubes, activated carbon, and zeolites. *Energy Fuels* **2008**, *22*, 3050–3056.
(23) Zelenak, V.; Madanicova, M.; Halamova, D.; Cejka, J.; Zukal, A.; Murafa, N.; Goerigk, G. Amine-modified ordered mesoporous silica: Effect of pore size on carbon dioxide capture. *Chem. Eng. J.* **2008**, *144*, 336–342.
(24) Arstad, B.; Fjellvag, H.; Kongshaug, K. O.; Swang, O.; Blom, R. Amine functionalized metal organic frameworks (MOFs) as adsorbents for carbon dioxide. *Adsorption* **2008**, *14*, 755–762.
(25) Lee, S.; Filburn, T. P.; Gray, M.; Park, J. W.; Song, H. J. Screening test of solid amine sorbents for CO_2 capture. *Ind. Eng. Chem. Res.* **2008**, *47*, 7419–7423.
(26) Son, W. J.; Choi, J. S.; Ahn, W. S. Adsorptive removal of carbon dioxide using polyethylenimine-loaded mesoporous silica materials. *Microporous Mesoporous Mater.* **2008**, *113*, 31–40.
(27) Kim, S. N.; Son, W. J.; Choi, J. S.; Ahn, W. S. CO_2 adsorption using amine functionalized mesoporous silica via anionic surfactant-mediated synthesis. *Microporous Mesoporous Mater.* **2008**, *115*, 497–503.
(28) Li, P.; Ge, B.; Zhang, S.; Chen, S.; Zhang, Q.; Zhao, Y. CO_2 capture by polyethylenimine-modified fibrous adsorbent. *Langmuir* **2008**, *24*, 6567–6574.
(29) Belmabkhout, Y.; Serna-Guerrero, R.; Sayari, A. Adsorption of CO_2-containing gas mixtures over amine-bearing pore-expanded MCM-41 silica. 1: Application to gas purification. *Ind. Chem. Eng. Res.* **2010**, *49*, 359–365.
(30) Chen, C.; Yang, S. T.; Ahn, W. S.; Ryoo, R. Amine-impregnated silica monolith with a hierarchical pore structure: Enhancement of CO_2 capture capacity. *Chem. Commun.* **2009**, 3627–3629.
(31) Vaidhyanathan, R.; Iremonger, S. S.; Dawson, K. W.; Shimizu, G. K. H. An amine-funtionalized metal organic framework for preferential CO_2 adsorption at low pressures. *Chem. Commun.* **2009**, 5230–5232.
(32) Serna-Guerrero, R.; Belmabkhout, Y.; Sayari, A. Further investigations of CO_2 using triamine-grafted pore expanded mesoporous silica. *Chem. Eng. J.* **2010**, *158*, 513–519.
(33) Filburn, T.; Helble, J. J.; Weiss, R. A. Development of supported ethanolamines and modified ethanolamines for CO_2 capture. *Ind. Eng. Chem. Res.* **2005**, *44*, 1542–1546.
(34) Plaza, M. G.; Pevida, C.; Arenillas, A.; Rubiera, F.; Pis, J. J. CO_2 capture by adsorption with nitrogen enriched carbons. *Fuel* **2007**, *86*, 2204–2212.
(35) Satyapal, S.; Filburn, T.; Trela, J.; Strange, J. Performances and properties of a solid amine sorbent for carbon dioxide removal in space life support application. *Energy Fuels* **2001**, *15*, 250–255.
(36) Choi, S.; Drese, J. H.; Jones, C. W. Adsorbent materials for carbon dioxide capture from large anthropogenic point sources. *ChemSusChem* **2009**, *2*, 796–854.

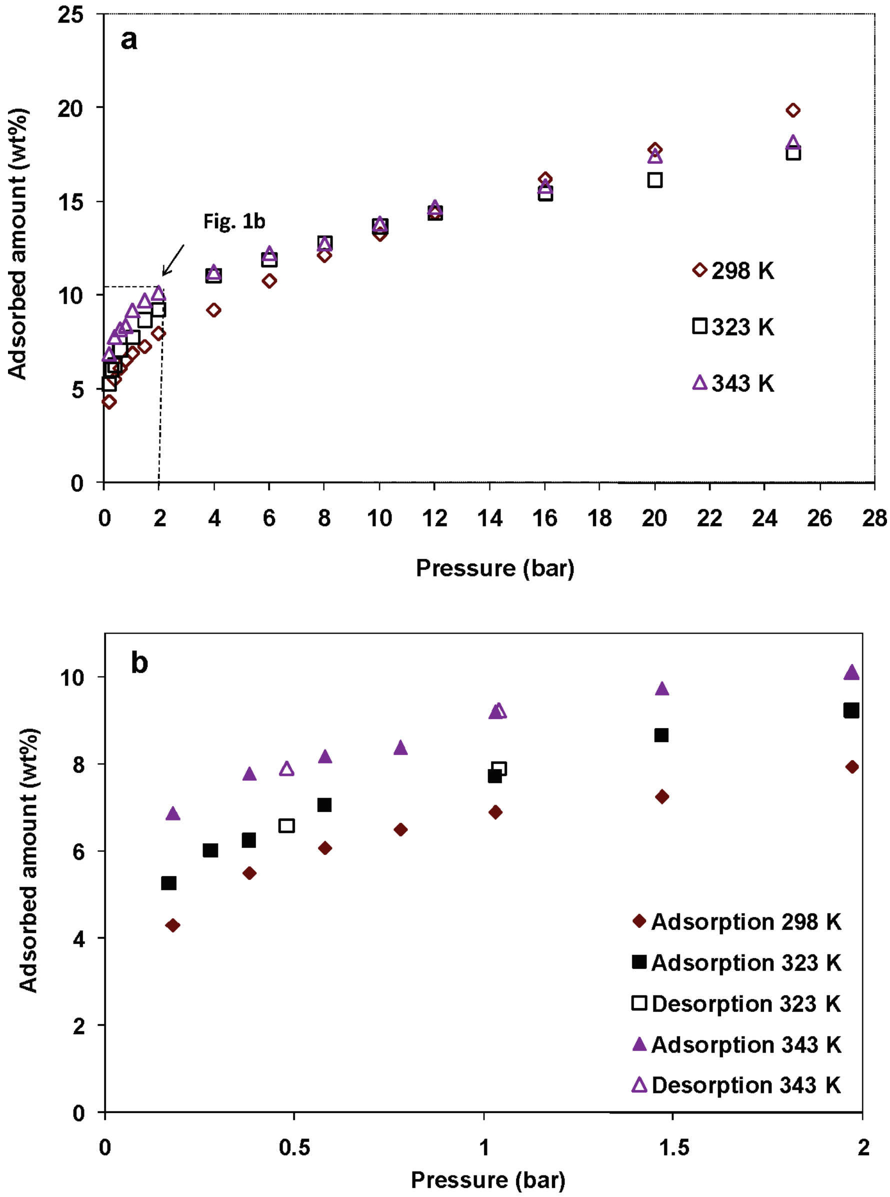

Figure 1. Adsorption isotherms of CO_2 on TRI-PE-MCM-41 at 298, 323, and 343 K: (a) adsorption up to 25 bar and (b) adsorption and desorption up to 2 bar.

at the same temperature as the adsorption temperature. More details about the experimental setup and procedure for the measurement of equilibrium adsorption isotherms may be found elsewhere.[12,18]

The procedure for cyclic measurements was as follows: the sample was first exposed to UHP nitrogen at 50 mL/min for 30 min at T (K) either under atmospheric pressure or 0.1 bar for CS and VS measurements, respectively. Subsequently, the feed gas was switched to pure CO_2 or 10:90 CO_2/N_2 at 50 mL/min at the same temperature. After 30 min of exposure, the desorption took place again under vacuum (VS) or atmospheric pressure (CS) at the same temperature under N_2 flowing at 50 mL/min for 30 min. The CO_2 working capacity (non-equilibrium) was assumed to be the weight gain of the sample after 30 min of exposure. For cyclic CO_2 adsorption−desorption experiments in the presence of moisture, the initial setup was slightly modified to allow the gas to pass continuously through a temperature-controlled saturator containing water. Because the desired level of moisture was maintained throughout the experiment, we assume that CO_2 is not displacing pre-adsorbed H_2O and that the CO_2 uptake corresponds to the weight gain during the adsorption step.

2.3. Column-Breakthrough Measurements for CO_2-Containing Binary Mixtures. The experimental setup used for dynamic column-breakthrough measurements was described elsewhere.[2]

2.4. Diffuse Reflectance Infrared Fourier Transform (DRIFT). A Nicolet Magna-IR 550 spectrometer equipped with a mercury cadmium telluride (MCT) detector and a Thermo diffuse reflectance cell was used to record DRIFT spectra. About 20 mg of powder sample was placed into the cell and pretreated in flowing ultra-high purity (UHP) He at 393 K for 2 h. The DRIFT spectra were then collected under a He atmosphere at 298 K. The spectrum for KBr was used as the background. The IR resolution was 4 cm^{-1}.

3. Results and Discussion

3.1. CO_2 Adsorption Isotherms. Figure 1a shows the adsorption isotherms of CO_2 on TRI-PE-MCM-41 up to 25 bar at 298, 323, and 343 K. The desorption data were omitted for clarity. At low to intermediate pressure (0−10 bar), the CO_2 uptake for TRI-PE-MCM-41 increased at increasing temperatures. Indeed, because of the strong

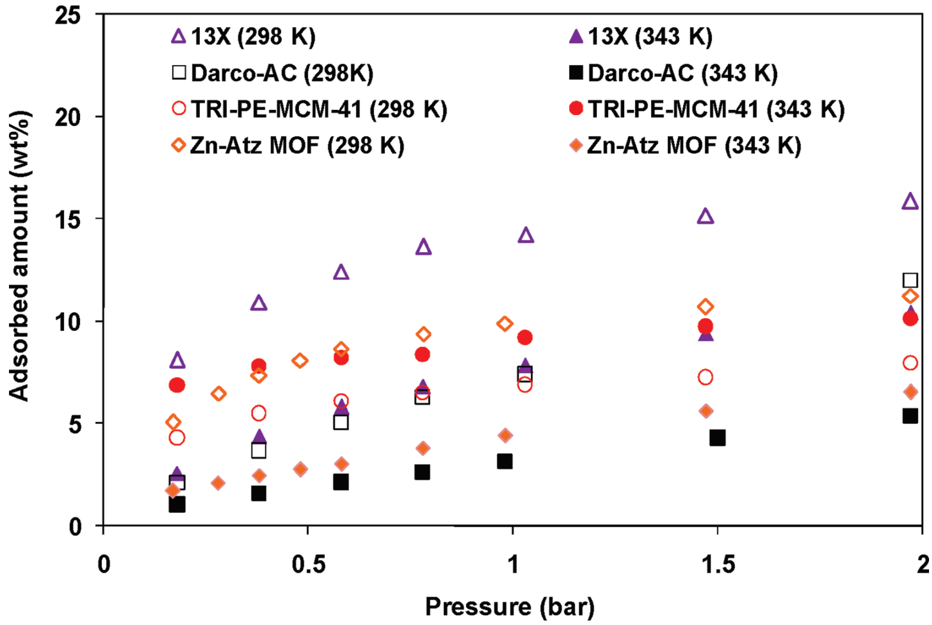

Figure 2. Adsorption isotherms of CO_2 up to 2 bar at 298 K (empty symbols) and 343 K (filled symbols) on TRI-PE-MCM-41, Zn-Atz MOF, 13X zeolite, and Darco-AC.

amine$-CO_2$ (from air) interactions, the number of available amine sites increases at increasing pretreatment temperatures from 298 to 343 K, leading to higher CO_2 uptake at higher temperatures. Notice that the temperature dependence of CO_2 uptake may change when a higher pretreatment temperature is applied. When the pretreatment temperature is high enough, e.g., 423 K (Figure S6 and S7 in the Supporting Information), the same total amount of amine sites is available and the actual CO_2 adsorption capacity decreases as the temperature increases. Moreover, as seen in Figure 1a, the sequence changed at high pressure because of the dominance of CO_2 physical adsorption.[18,37,38] Figure 1b represents a close-up of Figure 1a at low pressure (0−2 bar), including the desorption data. As seen, the CO_2 adsorption and desorption isotherms coincided for the 343 and 323 K isotherms but not in the case of 298 K (desorption isotherms at 298 K are not shown). This is most likely because, at such a low temperature, the CO_2 desorption rate was too low, so that the equilibrium criteria used, which corresponds to a mass change for less than 0.02 mg in 5 min, was met before a real equilibrium has been established.

Figure 2 shows the adsorption isotherms up to 2 bar for TRI-PE-MCM-41 at 298 and 343 K along with the adsorption isotherms for 13X, Zn-Atz MOF, and Darco-AC. At 298 K (for both adsorption and pretreatment), 13X outperformed TRI-PE-MCM-41, Zn-Atz MOF, and Darco-AC. However, when adsorption and pretreatment occurred at 343 K, TRI-PE-MCM-41 exhibited significantly higher CO_2 uptake than all of the other materials over the whole range of pressures. For example, at 0.2 bar, the uptake for TRI-PE-MCM-41 at 343 K was 6.82 wt % versus 2.64, 1.76, and 0.88 wt % for 13X, Zn-Atz MOF, and Darco-AC, respectively. Thus, TRI-PE-MCM-41 is more effective than the three other materials at high temperature. This may be advantageous for applications where the gas feed is supplied at high temperature, in the 308−343 K range.

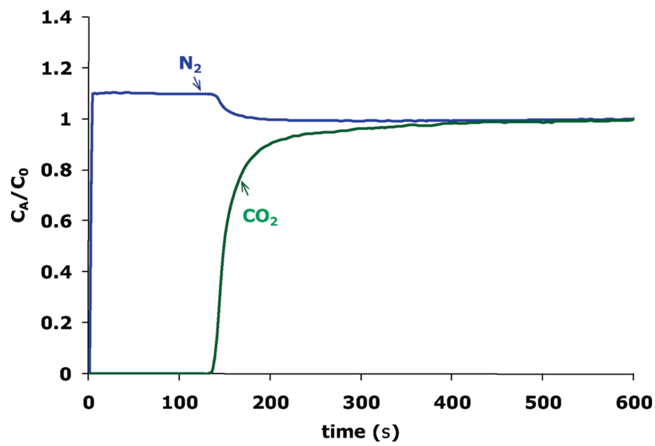

Figure 3. Column breakthrough data for 10:90 CO_2/N_2 at 343 K after pretreatment at 343 K in dry helium.

3.2. CO_2 Selectivity. For adsorption process efficiency, not only is the adsorption capacity important, but the CO_2 adsorption selectivity is also a key factor. Figure 3 shows the column-breakthrough curves for CO_2 and N_2 using a 10:90 CO_2/N_2 mixture akin to flue gas, at 343 K and 1 bar over TRI-PE-MCM-41 activated at 343 K. The amount of adsorbent was 0.45 g, and the flow rate was 100 mL/min. As seen, N_2 was detected downstream from the column immediately, indicating that the nitrogen uptake is negligible. The breakthrough time for CO_2 was 140 s. At saturation, the overall CO_2 dynamic adsorption uptake was ca. 1.46 ± 0.14 mmol/g (6.4 wt %). A capacity of ca. 1.52 ± 0.15 mmol/g (6.7 wt %) was obtained using a similar test with the pretreatment temperature of 373 K instead of 343 K (Figure S8 in the Supporting Information). In an earlier contribution, it was shown that CO_2 adsorption selectivity versus N_2 was exceedingly high at room temperature.[29] It is thus inferred that the selectivity of CO_2 over N_2 is very high, regardless of

(37) Serna-Guerrero, R.; Da'na, E.; Sayari, A. New insights into the interactions of CO_2 over amine-functionalized silica. *Ind. Eng. Chem. Res.* **2008**, *47*, 4761–4766.
(38) Bascik, Z.; Atluri, R.; Bennet-Garcia, A. E.; Hedin, N. Temperature-induced uptake of CO_2 and formation of carbamates in mesocaged silica modified with *n*-propylamines. *Langmuir* **2010**, *26*, 10013–10024.

the temperature of adsorption and pretreatment, within appropriate limits.

It was demonstrated elsewhere[39,40] that moisture in the feed enhances the CO_2 uptake at room temperature without adversity on CO_2 selectivity. To assess the effect of humidity on the CO_2 capture at a relatively higher temperature, a column-breakthrough experiment was carried out using a 10:90 CO_2/N_2 mixture with 7.5% relative humidity (RH) at 343 K and 1 bar (Figure S9 in the Supporting Information) and the data were compared to the corresponding findings in dry conditions (Figure S8 in the Supporting Information). The amount of adsorbent was 0.45 g, and the flow rate was 100 mL/min. As shown in Figure S9 in the Supporting Information, the N_2 uptake was negligible, leading to the inference that the selectivity of CO_2 over N_2 in the presence of humidity at 343 K is also very high. The breakthrough time for CO_2 was 155 s versus 140 s under dry conditions. Saturation of the bed occurred at a CO_2 dynamic adsorption uptake of ca. 1.55 ± 0.15 mmol/g (6.8 wt %). The breakthrough time for water vapor was 301 s, and the overall water uptake was 0.38 mmol/g (0.68 wt %), because of the combined contributions of physical adsorption and partial formation of bicarbonate.[37] Thus, 94.2% (6.4 wt %) and 5.8% (0.4 wt %) of adsorbed CO_2 are attributable to carbamate and bicarbonate formation, respectively. Using the reaction stoichiometry, the relative amount of adsorbed water at 343 K used for bicarbonate formation was 24% (0.09 mmol/g), with the rest (0.29 mmol/g) being physically adsorbed.

3.3. Adsorption−Desorption Cyclic Measurements. To assess the cyclability of TRI-PE-MCM-41 in the presence of pure CO_2 and a 10:90 CO_2/N_2 mixture, adsorption−desorption cyclic measurements were carried out using VS and CS regeneration modes at 298, 323, and 343 K. The data were compared to the corresponding measurements for 13X, Zn-Atz MOF, and Darco-AC. The adsorption−regeneration cycling was repeated 20 times for the two sets of desorption conditions. Using the same protocol, CS regeneration mode was also investigated in the presence of humid CO_2 and 10:90 CO_2/N_2 feeds over TRI-PE-MCM-41, 13X zeolite, and Darco-AC.

3.3.1. Adsorption of Pure CO_2. 3.3.1.1. Adsorption under Dry Conditions. Pure CO_2 cyclic adsorption−desorption measurements were carried out on TRI-PE-MCM-41 using VS and CS regeneration modes in dry conditions, where pretreatment, adsorption, and regeneration took place at the same temperature within the range of 298−343 K. Data associated with VS cycling are shown in Figure 4. The CO_2 uptake was fairly stable over 20 cycles when adsorption and desorption took place at 343 K. However, at 298 and 323 K, the CO_2 uptake decreased particularly during the first cycle before it leveled off. This behavior may be explained by the fact that, at low temperature, CO_2 does not desorb completely, indicating that a relatively constant amount of CO_2 was withheld upon regeneration.

As shown in Figure 5, CS cycles exhibited qualitatively the same behavior as VS cycles; however, a more significant loss in CO_2 capacity was observed after the first adsorption−desorption cycle at 298 K (67 versus 20%) and 323 K

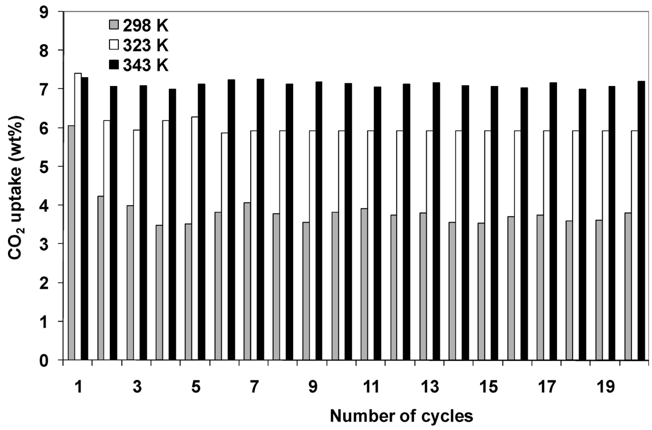

Figure 4. CO_2 uptake during cycling of pure CO_2 over TRI-PE-MCM-41 using VS regeneration mode at different temperatures.

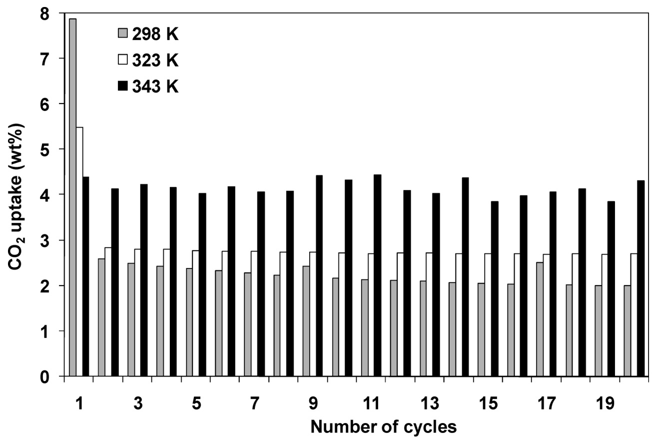

Figure 5. CO_2 uptake during cycling of pure CO_2 over TRI-PE-MCM-41 using CS regeneration mode at different temperatures.

(48 versus 16%). As in the case of VS(343) cycles, no loss was observed for CS(343) cycles. Because under otherwise the same conditions, vacuum provides a stronger driving force for desorption, the working CO_2 uptake was higher for VS than CS cycling. Notice that, for pure CO_2, VS(343) cycling exhibited 32 and 23% lower CO_2 uptake than TVS(323-0.1-363) and TS(323-1-363) configuration modes, respectively (Figure S1 in the Supporting Information).

Adsorption data for pure CO_2 over TRI-PE-MCM-41 during VS and CS cycling under dry conditions along with similar measurements in the presence of 13X, Zn-Atz MOF, and Darco-AC at 298 and 343 K are shown in Figures 6 and 7. With regard to VS cycles, 13X, Zn-Atz MOF, and Darco-AC exhibited stable adsorption uptake over the 20 cycles for both temperatures, whereas at 298 K, TRI-PE-MCM-41 showed some decrease in CO_2 uptake at the first cycle. At 298 K, 13X significantly outperformed all other adsorbents and the sequence for CO_2 uptake was 13X > Zn-Atz MOF > Darco-AC > TRI-PE-MCM-41. However at 343 K, TRI-PE-MCM-41 showed comparable performance to 13X, while Darco-AC became the least effective following the sequence TRI-PE-MCM-41 ≥ 13X > Zn-Atz MOF > Darco-AC. Figure S2 in the Supporting Information shows that when TVS(323-0.1-363) cycling is applied for pure CO_2, the sequence was 13X > TRI-PE-MCM-41 > Zn-Atz MOF.

As for CS cycling, at 298 K, TRI-PE-MCM-41 exhibited very low capacity of ca. 2 wt %, because of a drastic decrease

(39) Belmabkhout, Y.; De Weireld, G.; Sayari, A. Amine bearing mesoporous silica for CO_2 and H_2S removal form natural gas and biogas. *Langmuir* **2009**, *25*, 13275–13278.
(40) Belmabkhout, Y.; Serna-Guerrero, R.; Sayari, A. Amine bearing mesoporous silica for CO_2 removal from dry and humid air. *Chem. Eng. Sci.* **2010**, *65*, 3695–3698.

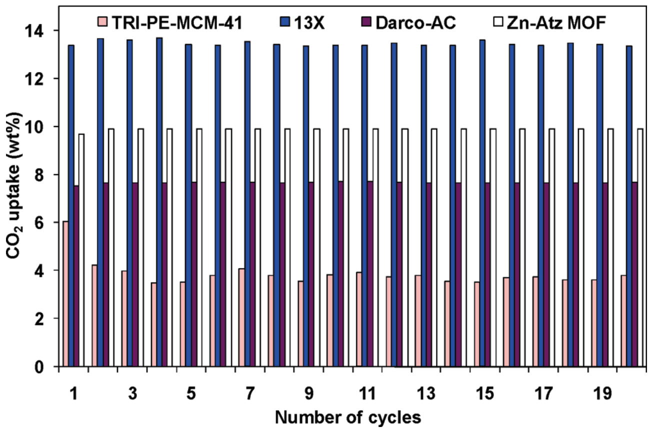

Figure 6. CO_2 uptake during pure CO_2 cycling on TRI-PE-MCM-41, 13X, and Darco-AC using VS regeneration at 298 K.

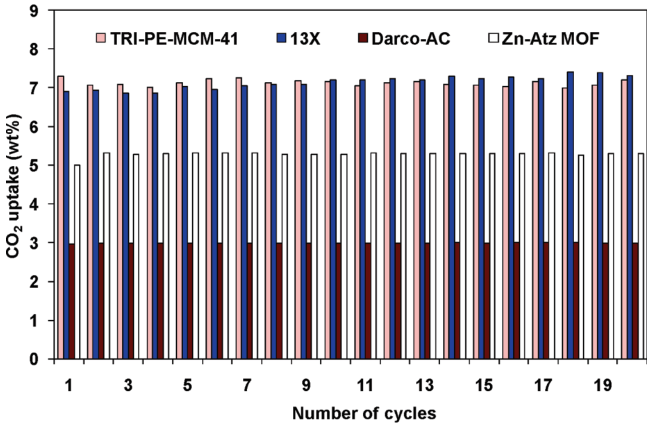

Figure 7. CO_2 uptake during pure CO_2 cycling on TRI-PE-MCM-41, 13X, and Darco-AC using VS regeneration at 343 K.

(67%) after the first cycle, most likely because of incomplete regeneration (Figure 8). Notice that 13X also showed a 37% decrease after the first cycle. The sequence of CO_2 uptake at room temperature was 13X ≫ Darco-AC > TRI-PE-MCM-41. At 343 K, TRI-PE-MCM-41 exhibited higher CO_2 uptake than Darco-AC but was still ca. 36% lower than 13X. For all materials, no significant decrease in the CO_2 uptake was observed at 343 K over 20 cycles. The sequence in terms of CO_2 adsorption capacity was 13X > TRI-PE-MCM-41 > Darco-AC. Thus, when using pure CO_2 in dry conditions, TRI-PE-MCM-41 exhibits lower capacity than 13X using CS regeneration mode at both 298 and 343 K. However, it is worthy to note that, in the case of VS cycling, the CO_2 uptake for TRI-PE-MCM-41 at 343 K was 47% higher than at 298 K, whereas the CO_2 uptake for 13X zeolite and Darco-AC droped by 45 and 60%, respectively.

3.3.1.2. Adsorption in the Presence of Moisture. In actual adsorption separation processes, the gas feed often contains different amounts of water vapor, resulting in additional downstream complexity, which could be mitigated if the adsorbent is water-tolerant. The effect of water vapor on the performance of TRI-PE-MCM-41 was investigated using the CS regeneration mode. Because of difficulties to control the level of moisture under vacuum, VS cycling was not undertaken. Figure 9 shows 20 CS cycles on TR-PE-MCM-41, 13X, and Darco-AC at 343 K using CO_2 with 7.5% RH. In the first cycles, the sequence of CO_2 uptake was

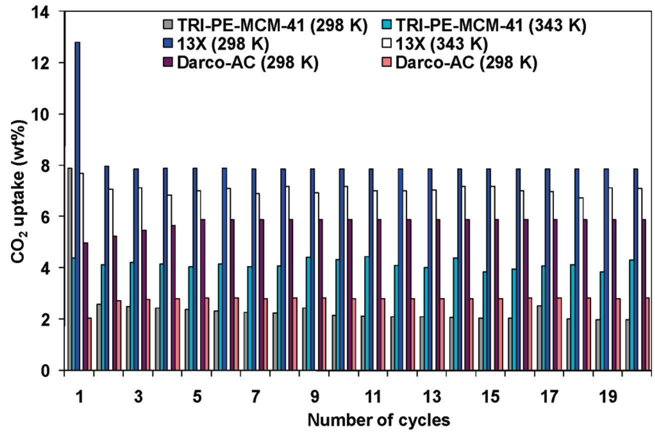

Figure 8. CO_2 uptake during pure CO_2 cycling on TRI-PE-MCM-41, 13X, and Darco-AC using CS regeneration mode at 298 and 343 K.

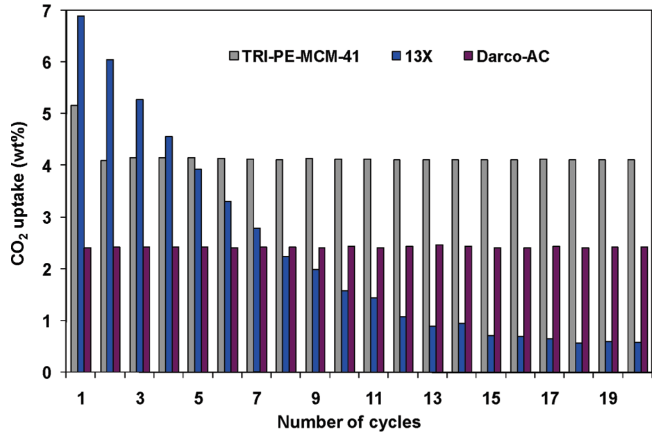

Figure 9. CO_2 uptake during cycling of pure CO_2 with 7.5% RH on TRI-PE-MCM-41, 13X, and Darco-AC using CS regeneration mode at 343 K.

13X > TRI-PE-MCM-41 > Darco-AC. However, the performance of 13X deteriorated dramatically in the presence of moisture, with 90% loss after 20 cycles, leading to the following order of CO_2 capture TRI-PE-MCM-41 ≫ Darco-AC > 13X. This was attributed to the high affinity of 13X for water in comparison to CO_2, as pointed out by others.[41−43] Darco-AC lost 12% of CO_2 uptake in the presence of moisture in comparison to its performance under dry conditions (Figure 7) but remained stable. Although under dry conditions, the CS cycling did not seem to be suitable for TRI-PE-MCM-41, this material outperformed 13X and Darco-AC in the presence of moisture. The effect of moisture on TRI-PE-MCM-41 and 13X under TS(323-1-363) regeneration mode is discussed in Figure S3 in the Supporting Information.

It is important to notice that, in contrast to TRI-PE-MCM-41, some nitrogen used as the purge gas during regeneration may adsorb on 13X and Darco-AC. Thus, the

(41) Brandani, F.; Ruthven, D. The effect of water on the adsorption of CO_2 and C_3H_8 on type X zeolites. *Ind. Eng. Chem. Res.* **2004**, *43*, 8339–8344.
(42) Bonenfant, D.; Kharoune, M.; Niquette, P.; Mimeault, M.; Hausler, R. Advances in principal factor influencing carbon dioxide adsorption in zeolites. *Sci. Technol. Adv. Mater.* **2008**, *9*, 013001–013007.
(43) Stevens, R. W., Jr.; Siriwardane, R. V.; Logan, J. In situ Fourier transform infrared spectra (FTIR) investigation of CO_2 adsortion onto zeolite materials. *Energy Fuels* **2008**, *22*, 3070–3079.

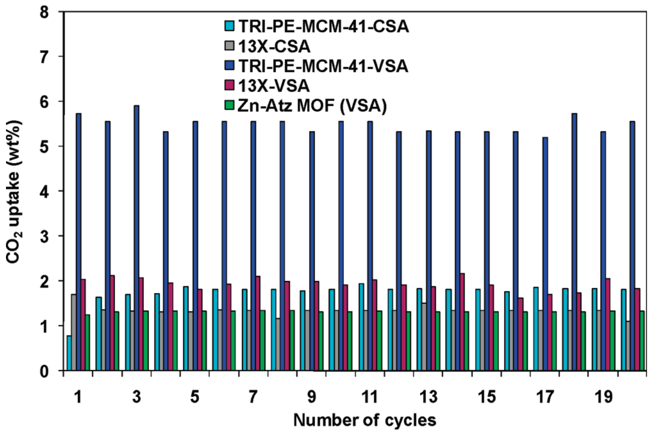

Figure 10. VS and CS cycles using a 10:90 CO_2/N_2 mixture at 343 K on TRI-PE-MCM-41, 13X, and Zn-Atz MOF in dry conditions.

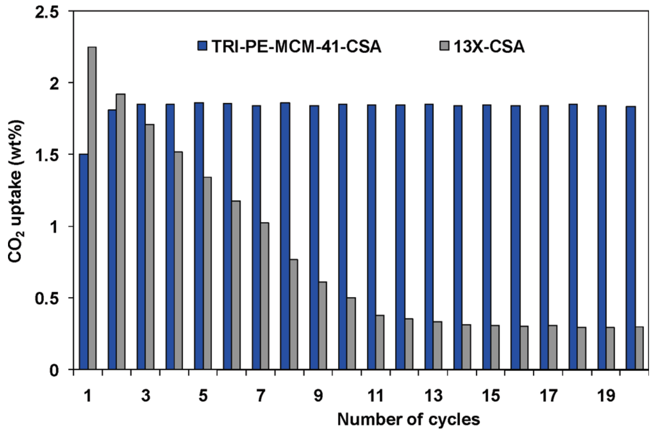

Figure 11. CS cycles using a 10:90 CO_2/N_2 mixture at 343 K on TRI-PE-MCM-41 and 13X in humid conditions (7.5% RH).

CO_2 uptake over these two adsorbents may have been slightly underestimated because some CO_2 may have displaced nitrogen without being detected by the gravimetric measurements. However, with the N_2 adsorption capacity at 1 bar (at 298 and 343 K) over 13X zeolite and Darco-AC being quite small, the assumption that the weight gain during the adsorption stage corresponds to the CO_2 adsorption uptake is justified.

3.3.2. 10:90 CO_2/N_2 Mixture. Because some key adsorption properties, such as CO_2 selectivity, may be overlooked when screening is based on pure CO_2, similar VS and CS cyclic measurements were carried out in the presence of a 10:90 CO_2/N_2 mixture in both dry and humid conditions.

3.3.2.1. Adsorption under Dry Conditions. Figure 10 shows VS and CS cyclic measurements on TRI-PE-MCM-41, 13X, and Zn-Atz MOF carried out using a 10:90 CO_2/N_2 mixture at 343 K. Interestingly, in terms of CO_2 uptake, the observed trend was not the same as for pure CO_2. TRI-PE-MCM-41 significantly outperformed 13X and Zn-Atz MOF when VS regeneration mode was applied, while comparable performances were observed for CS regeneration. This behavior stems from the extremely high CO_2 selectivity of TRI-PE-MCM-41 in comparison to 13X and Zn-Atz MOF. Figure S4 in the Supporting Information also shows that, using TVS(323-0.1-363) cycling, TRI-PE-MCM-41 largely outperformed 13X and Zn-Atz MOF. Thus, using a CO_2 concentration akin to flue gas, TRI-PE-MCM-41 exhibited better performances than 13X zeolite and Zn-Atz MOF even in dry conditions. The cyclic CO_2 adsorption capacity in the case of VS(343) regeneration mode was similar to TS(323-1-363) shown in Figure S5 in the Supporting Information and only ca. 12% lower than the cyclic CO_2 adsorption capacity associated with TVS(323-0.1-363) mode.

3.3.2.2. Adsorption in the Presence of Moisture. Figure 11 shows CS cyclic measurements on TRI-PE-MCM-41 and 13X carried out using a 10:90 CO_2/N_2 mixture with 7.5 RH at 343 K to study the effect of humidity on working CO_2 uptake. Similar to pure CO_2, the CO_2 uptake on 13X decreased dramatically in the presence of moisture, by ca. 86% after 20 cycles, while the uptake over TRI-PE-MCM-41 was stable and unchanged compared to the dry conditions. It is worth mentioning that the VS CO_2 uptake for TRI-PE-MCM-41 at 343 K is expected to be at least the same as in dry conditions, i.e., 6 and 7 wt %, respectively, for a 10:90 CO_2/N_2 mixture and pure CO_2. This is of prime importance because no gas drying will be required prior to the removal of CO_2 using TRI-PE-MCM-41. The corresponding effect of moisture in the case of TS(323-1-363) regeneration mode is discussed in Figure S5 in the Supporting Information. In addition, as shown recently,[44] the occurrence of moisture in the gas streams dramatically increased the stability of TRI-PE-MCM-41, allowing more than 700 CS(343) cycles to be achieved without any loss in CO_2 adsorption capacity.

3.3.3. Effect of Typical Impurities on CO_2 Adsorption. Water vapor and O_2 are ubiquitous impurities in flue gas. However, as demonstrated elsewhere,[29] the adsorptive properties are not affected in any way by the presence of oxygen, whereas water vapor has a positive effect on the adsorption of CO_2, because of the partial formation of ammonium bicarbonate with a CO_2/N stoichiometric ratio of 1, instead of carbamate with $CO_2/N = 0.5$.[37] Dependent upon the nature of the fossil fuel and the gas pretreatment, flue gas may contain traces of sulfur-containing species, particularly SO_2. Diaf et al.[46] reported that SO_2 adsorption over co-polymers modified by tertiary amines or ethylenediamine-modified co-polymers was essentially reversible. However, Khatri et al.[47] showed that SO_2 adsorbs irreversibly on propylamine-grafted SBA-15. To investigate the effect of traces of SO_2 on CO_2 adsorption over TRI-PE-MCM-41 (one primary and two secondary amines), a fresh sample was loaded in the Rubotherm microbalance, activated under vacuum at 373 K, then cooled to 323 K, and exposed to 10% CO_2/N_2. The amount of CO_2 adsorbed was ca. 6.9 wt %. The material was regenerated under vacuum at 373 K for 2 h and exposed to 0.23 mbar of pure SO_2 at 323 K. A SO_2 adsorption equilibrium capacity of 1.18 wt % was obtained. On the basis of the weight change, after the sample was treated at 373 K under vacuum for 2 h, only 85% of SO_2 was desorbed.

Nonetheless, the sample was exposed again to 10% CO_2/N_2 at 323 K. The equilibrium adsorption capacity was only

(44) Sayari, A.; Belmabkhout, Y. Stabilization of amine-containing CO_2 adsorbents: Dramatic effect of water vapor. *J. Am. Chem. Soc.* **2010**, *132*, 6312–6314.
(45) Xu, X.; Song, C.; Miller, B. G.; Scaroni, A. W. Adsorption separation of carbon dioxide from flue gas-fired boiler by a novel nanoporous "molecular basket" adsorbent. *Fuel Process. Technol.* **2005**, *86*, 1457–1472.
(46) Diaf, A.; Garcia, J. L.; Beckman, E. J. Thermally reversible polymeric sorbents for acid gases. CO_2, SO_2 and NO_x. *J. Appl. Polym. Sci.* **1994**, *53*, 857–874.
(47) Khatri, A. R.; Chuang, S. S. C.; Soong, Y.; Gray, M. Thermal and chemical stability of regenerable solid amine sorbent for CO_2 capture. *Energy Fuels* **2006**, *20*, 1514–1520.

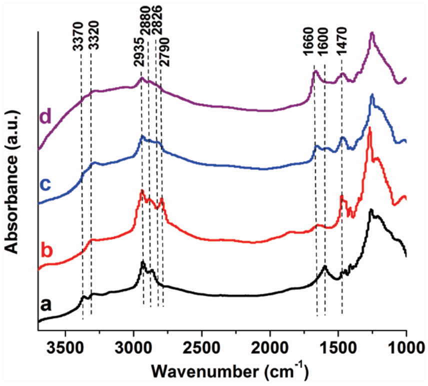

Figure 12. DRIFT spectra for (a) fresh propylamine-grafted PE-MCM-41, (b) fresh *N*-methylpropylamine-grafted PE-MCM-41, (c) fresh TRI-PE-MCM-41, and (d) TRI-PE-MCM-41 after exposure to traces of SO_2.

3.9 wt % of CO_2 versus 6.9 wt % for the fresh material. The irreversible loss of CO_2 adsorption uptake upon exposure of the material to traces of SO_2 may be associated with the formation of thermally stable salts.[45] Figure 12 shows DRIFT spectra of TRI-PE-MCM-41 before (Figure 12c) and after (Figure 12d) exposure to SO_2. The main change is the disappearance of the band at ca. 1600 cm^{-1}. A comparison to the DRIFT spectra of fresh propylamine-grafted PE-MCM-41 (Figure 12a) and *N*-methylpropylamine-grafted PE-MCM-41 (Figure 12b) shows that 1600 cm^{-1} is associated with the NH_2 deformation of primary amine.[48,49] Thus, we tentatively assign the loss of CO_2 adsorption capacity of TRI-PE-MCM-41 upon exposure to SO_2 to irreversible interactions with the primary amine groups. Further effort is underway to delineate the nature of the amine−SO_2 interactions and mitigate or circumvent such a negative effect.

(48) Chang, F. Y.; Chao, K. J.; Cheng, H. H.; Tan, C. S. Adsorption of CO_2 onto amine-grafted mesoporous silicas. *Sep. Purif. Technol.* **2009**, *70*, 87–95.
(49) Hiyoshi, N.; Yogo, K.; Yashima, T. Adsorption characteristics of carbon dioxide on organically functionalized SBA-15. *Microporous Mesoporous Mater.* **2005**, *84*, 357–365.

4. Conclusion

This work dealt with the potential feasibility of vacuum or concentration swing adsorption for CO_2 capture from flue gas over amine-bearing pore-expanded MCM-41. Using the same temperature for pretreatment and adsorption, TRI-PE-MCM-41 exhibited at 343 K, higher equilibrium uptake than 13X, Zn-Atz MOF, and Darco-AC. Moreover, column-breakthrough experiments showed very high selectivity toward CO_2 in the presence of a 10:90 CO_2/N_2 mixture. Measurements using VS regeneration mode showed that TRI-PE-MCM-41 can be cycled with ca. 5.9 wt % uptake in the presence of a 10:90 CO_2/N_2 mixture at 343 K versus 6.7 wt % for TS(323-1-363). Thus, CO_2 removal from flue gas over TRI-PE-MCM-41 as an adsorbent may be carried out using VSA without any drying, heating, cooling, or compression prior to separation. It was also demonstrated that SO_2 has an adverse effect on CO_2 adsorption over TRI-PE-MCM-41, and its removal prior to CO_2 adsorption is required. Further effort to mitigate the effect of SO_2 is underway.

Acknowledgment. We thank co-worker Rodrigo Serna-Guerrero for providing the column-breakthrough data and Yong Yang for preparing the MOF sample. The financial support of the Natural Science and Engineering Council of Canada (NSERC) is acknowledged. Y.B. thanks NSERC for a postdoctoral fellowship. A.S. thanks the Federal Government for the Canada Research Chair in Nanostructured Materials for Catalysis and Separation (2001−2015).

Supporting Information Available: Adsorption isotherms, TS and TVS cycling procedure, CO_2 adsorption−desorption cyclic data using TS and TVS, and column-breakthrough measurements. This material is available free of charge via the Internet at http://pubs.acs.org.